

Chemistry of Electrolyte Reduction on Lithium Silicide

Yun Xu, Kevin Wood, Jaclyn Coyle, Chaiwat Engrakul, Glenn Teeter, Conrad R. Stoldt, Anthony Burrell, and Andriy Zakutayev

J. Phys. Chem. C, **Just Accepted Manuscript** • DOI: 10.1021/acs.jpcc.9b02611 • Publication Date (Web): 07 May 2019

Downloaded from <http://pubs.acs.org> on May 16, 2019

Just Accepted

“Just Accepted” manuscripts have been peer-reviewed and accepted for publication. They are posted online prior to technical editing, formatting for publication and author proofing. The American Chemical Society provides “Just Accepted” as a service to the research community to expedite the dissemination of scientific material as soon as possible after acceptance. “Just Accepted” manuscripts appear in full in PDF format accompanied by an HTML abstract. “Just Accepted” manuscripts have been fully peer reviewed, but should not be considered the official version of record. They are citable by the Digital Object Identifier (DOI®). “Just Accepted” is an optional service offered to authors. Therefore, the “Just Accepted” Web site may not include all articles that will be published in the journal. After a manuscript is technically edited and formatted, it will be removed from the “Just Accepted” Web site and published as an ASAP article. Note that technical editing may introduce minor changes to the manuscript text and/or graphics which could affect content, and all legal disclaimers and ethical guidelines that apply to the journal pertain. ACS cannot be held responsible for errors or consequences arising from the use of information contained in these “Just Accepted” manuscripts.



Chemistry of Electrolyte Reduction on Lithium Silicide

*Yun Xu,^[a] Kevin Wood,^[a] Jaclyn Coyle,^[a] Chaiwat Engtrakul,^[a] Glenn Teeter,^[a] Conrad
Stoldt,^[b] Anthony Burrell,^[c] Andriy Zakutayev*^[a]*

[a] Materials Science Center, National Renewable Energy Laboratory, Golden, CO,
80401, USA

[b] Materials Science & Engineering Program, University of Colorado Boulder,
Boulder, CO, 80309, USA

[c] Chemistry and Nanoscience Center, National Renewable Energy Laboratory,
Golden, CO, 80401, USA

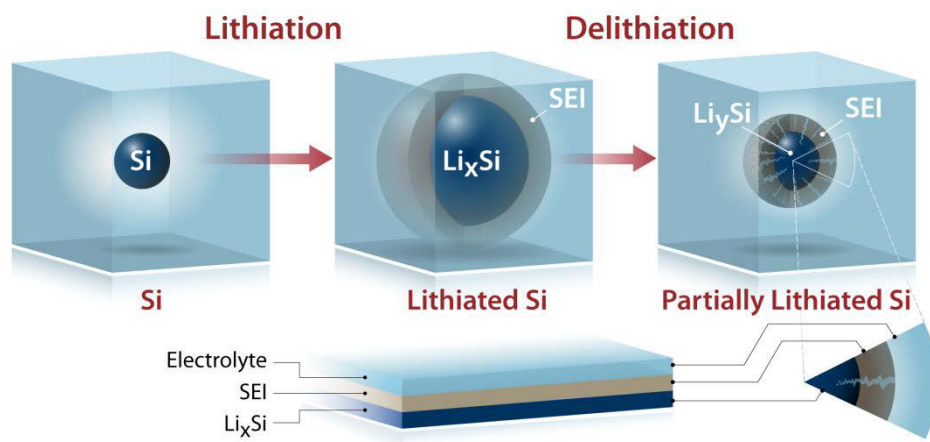
ABSTRACT: Silicon anodes are promising for next-generation lithium-ion batteries due to high theoretical capacity. However, their performance and lifetime are currently limited by continuous electrolyte reduction and solid-electrolyte interphase (SEI) formation. Thus, SEI studies are important, but often complicated due to the rough morphology of samples, buried interfaces, and presence of binders. Here, we demonstrate the chemical origin of SEI formation by electrolyte reduction on lithium

1
2
3 silicide thin films, synthesized by diffusion of pure evaporated lithium into smooth
4
5
6 sputtered silicon. These model samples allowed for accurate estimation of irreversible
7
8
9 capacity loss due to electrolyte reduction and for precise characterization of the resulting
10
11 SEI by vibrational and photoelectron spectroscopies. Spectroscopic characterizations
12
13
14 showed clear evidence that lithium silicide reduced electrolyte directly upon contact.
15
16
17 Negligible first-cycle irreversible capacity loss was observed for the lithium silicide
18
19
20 compared to silicon, indicating that the decomposition product of electrolyte on lithium
21
22
23 silicide is able to stop further electrolyte reduction to a large extent. Fluoro-ethylene
24
25 carbonate (FEC) was shown to significantly affect the chemistry of electrolyte reduction
26
27
28 on lithium silicide and subsequent cycling performance. The results of this basic study
29
30
31 reveal the chemistry occurring at the interface of the lithium silicide and electrolyte and
32
33
34 help in understanding the limited calendar lifetime of Li-ion batteries with Si anodes.
35
36

37 **Introduction**

38
39
40
41 Silicon is one of the most promising alternatives to graphite anodes in rechargeable
42
43
44 lithium-ion batteries due to its high theoretical capacity of 4,200 mAh/g.¹ If realized, such
45
46
47 high capacity would be in great demand for consumer electronics and electric vehicles.
48
49
50 Despite this attractive feature, to date, Si anodes have not been commercialized because
51
52
53 of several technological problems.² In the first cycle, active Li ions are consumed due to
54
55
56 1) the solid-electrolyte interphase (SEI) film formation, which leads to irreversible
57
58
59
60

1
2
3 capacity loss, and 2) much lower first-cycle coulombic efficiency compared to graphite.
4
5
6 Even more importantly, as shown in Figure 1, continuous electrolyte consumption occurs
7
8 in subsequent cycles, when cracks form and fresh surfaces are exposed to the electrolyte.
9
10
11 This continuous consumption of electrolyte ultimately leads to battery degradation.
12
13
14 Overall, these challenges compromise the application of Si anodes in batteries.
15



16
17
18
19
20
21
22
23
24
25
26
27
28
29
30
31
32 **Figure 1.** Schematic illustration of crack formation on Si anode upon cycling, and fresh
33
34 Li_xSi surface exposure to electrolyte when cracks form. A thin-film model is used to study
35
36 the interface and interphase between lithium silicide and electrolyte.
37
38
39

40
41 To address these applied technological problems, a basic scientific understanding of
42
43 SEI formation is crucial. To this end, numerous studies of SEI formation on
44
45 electrochemically lithiated silicon have been conducted using X-ray photoelectron
46
47 spectroscopy (XPS),³ nuclear magnetic resonance (NMR),⁴ X-ray diffraction (XRD),⁵
48
49 neutron reflectometry (NR),⁶ Fourier-transform infrared spectroscopy (FTIR),⁷⁻⁸ atomic-
50
51 force microscopy (AFM),⁹ and more. Despite significant progress in understanding, such
52
53
54
55
56
57
58
59
60

1
2
3 electrochemical studies are often complicated by the rough sample morphology, buried
4
5
6 nature of the Li_xSi /electrolyte interface, presence of binders used for electrochemical
7
8
9 lithiation of silicon, and other factors (Figure 1). Thus, what forms at the Li_xSi /electrolyte
10
11
12 interface and what these interphases do to the anode performance are still largely
13
14 unknown.¹⁰⁻¹¹ Answering these questions may have important implications for
15
16
17 improving the limited calendar and cycle lifetimes of Li-ion batteries with Si anodes.
18

19
20 An alternative approach to understanding what happens to fresh exposed lithium
21
22 silicide at cracks is to expose chemically synthesized lithium silicide to the electrolyte and
23
24
25 study the chemical reaction products. All common electrolyte components—such as
26
27
28 ethylene carbonate (EC), dimethyl carbonate (DMC),^{12,13} and fluoro-ethylene carbonate
29
30 (FEC) additive^{14,15}—have reduction potentials of 0.7–1.3 V, which is much higher than
31
32
33 that of lithium silicide. Thus, all these electrolyte components should be possible to
34
35
36 reduce by this simple chemical reaction. Despite considerable experimental work on the
37
38
39 electrochemical electrolyte decomposition on Si,¹⁶⁻¹⁹ no experimental studies on chemical
40
41
42 electrolyte reduction have been reported. Several computational papers are available on
43
44
45 chemical reduction of electrolyte components on the lithium silicide surface,^{20 21} but
46
47
48 similar experimental studies are missing from the literature. One major challenge in
49
50
51 synthesis and characterization of lithium silicide is the strong reactivity of these materials
52
53
54 with oxygen. In particular, Li is a very electropositive element with an electronegativity
55
56
57 of 1. Thus, significant contamination (e.g., 20% from XPS depth profile²²) can occur even
58
59
60

1
2
3 if very little oxygen is present in the synthesis or characterization equipment, or during
4
5
6 the sample transfer.
7

8
9 Here, we report on the experimental study of the chemistry of electrolyte reduction on
10
11 lithium silicide. For this purpose, nearly oxygen-free lithium silicide samples with planar
12
13 geometry were prepared by diffusion of evaporated lithium into sputtered silicon thin
14
15 film. The smooth surface of these samples enabled accurate spectroscopic
16
17 characterization of the SEI to elucidate the effect of electrolyte composition on the
18
19 reduction products. These model system samples also enabled quantitative
20
21 electrochemical evaluation of irreversible capacity and estimation of electrolyte
22
23 consumption in the first cycle, found to be negligible for lithium silicide compared to
24
25 silicon. The results of these studies indicate that electrolyte reduction on lithium silicide
26
27 occurs by a purely chemical reaction and suggests a possibility of forming SEI on
28
29 prelithiated silicon for improved cell cycling performance.
30
31
32
33
34
35
36
37

38 **Experimental Section**

39
40

41 Lithium silicide thin films were synthesized in a two-step process. First, a 50-nm silicon
42
43 thin film was deposited by RF magnetron sputtering at 4.5 W/cm² from a 99.999%-pure,
44
45 2-inch Si target positioned 8 cm away from the Cu foil and Pt/Si substrates in 5×10⁻³ torr
46
47 of Ar. Second, a 200-nm lithium thin film was thermally evaporated onto the silicon thin
48
49 film at a rate of 2 Å/s and monitored by a quartz-crystal microbalance. Both depositions
50
51 were performed in a vacuum chamber with a base pressure of 3×10⁻⁸ torr coupled to a
52
53
54
55
56
57
58
59
60

1
2
3 glovebox (0.1 ppm of O₂). Following the depositions steps, lithium silicide was formed
4
5
6 by inter-diffusion of lithium into silicon at ambient conditions driven by the high
7
8
9 chemical potential of lithium on the silicon surface.

10
11 Two types of electrolytes were used in this study. The first electrolyte was composed
12
13 of LiPF₆ (1.2M) dissolved in EC+DMC (volume ratio = 3:7). The second electrolyte also
14
15 contained FEC (10 wt.%). For galvanostatic charge and discharge cycling measurements in
16
17 coin cells, lithium silicide thin films on Cu foil with 15-mm diameter were assembled with
18
19 lithium foil as a reference electrode. These half-cells were discharged to 50 mV and
20
21 charged to 1 V at a C/5 rate. In addition, these two electrolytes were dropped on the
22
23 surface of the lithium silicide thin film deposited on a Pt-coated silicon wafer for the
24
25 attenuated total reflection – Fourier-transform infrared spectroscopy (ATR-FTIR)
26
27 measurements. After 20 min of exposure, DMC solvent was used to gently wash the
28
29 sample. The ATR-FTIR was performed with a Bruker Alpha spectrometer in a glovebox
30
31 under argon atmosphere. Peak analysis was based on previous ATR-FTIR studies^{6, 23} of
32
33 SEI formation on lithium and silicon.
34
35
36
37
38
39
40
41
42
43

44 The XPS measurements were performed using a glovebox-integrated Phi 5600 XPS
45
46 system. Glovebox conditions were better than <10 ppm H₂O and O₂. Base pressures for
47
48 the XPS system were below 7×10⁻¹⁰ torr. Photoelectrons were generated using
49
50 monochromatic Al Kα X-ray excitation (1,486.7 eV). The spectrometer binding-energy
51
52 (BE) scale was calibrated by measuring valence-band and core-level spectra from sputter-
53
54
55
56
57
58
59
60

cleaned Au, Ag, and Cu foils ($E_F = 0.00$ eV, Au 4f7/2 = 83.96 eV, Ag 3d5/2 = 368.26 eV, and Cu 2p3/2 = 932.62 eV). Ar⁺ sputtering (incident energy 3 keV) was used for depth profiling. Curve fitting and data processing were performed using Igor Pro with a custom program adapted from Schmid et al.²⁴

Results and Discussions

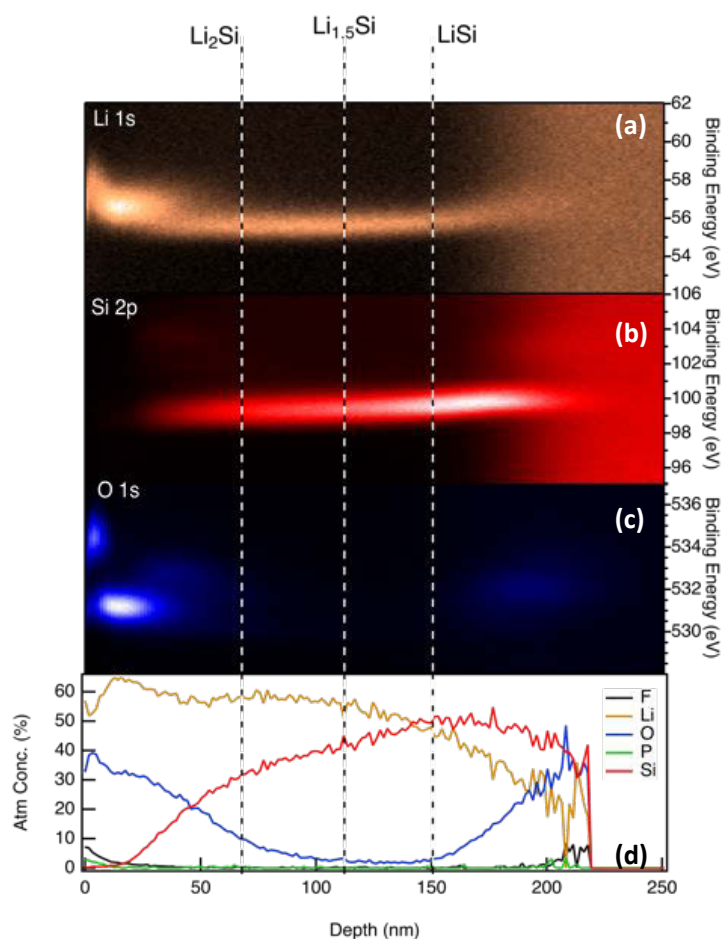
Table 1. Comparison of oxygen contamination and lithium content determined from XPS measurements for two different lithium silicide deposition techniques

Deposition Technique	Pressure (torr)	Li rate (Å/s)	O (at%)	Li (at%)	Si (at%)
Li / Si co-sputtering	5×10^{-3}	0.5	40	20	40
Si sputtering / Li evaporation	4×10^{-8}	2	1	~50	~50

As shown in Table 1, a combined sputtering/thermal evaporation technique resulted in lithium silicide thin films with much lower oxygen levels (~1% in the bulk) compared to our previous work²⁵ on Li_xSiO_y thin films obtained by a Li/Si co-sputtering method. One possible reason for lower oxygen content is the high vacuum environment of the Li evaporation process (4×10^{-8} torr base pressure, mostly water vapor) compared to Li sputtering (5×10^{-3} torr of Ar). Another likely reason is that Li evaporation lacks the presence of Ar plasma that is used for sputtering, which can make oxygen (resulting from

Pursuant to the DOE Public Access Plan, this document represents the authors' peer-reviewed, accepted manuscript. The published version of the article is available from the relevant publisher.

the water-vapor base pressure in the chamber) more reactive. Finally, the Li deposition rate in thermal evaporation was four times higher than that in sputtering due to an upper limit of power that can be applied to the Li sputtering target before causing it to melt. The higher vacuum environment, higher deposition rate, and absence of plasma during Li evaporation all helped to reduce oxygen contamination in the lithium silicide thin films reported here. In addition to reducing the oxygen contamination, the combined sputtering/evaporation technique also led to thin-film samples with higher lithium content, as shown in Table 1.



1
2
3 **Figure 2.** XPS color-intensity maps showing the signal intensity and binding energy of
4 (a) Li 1s, (b) Si 2p, and (c) O 1s as a function of distance from the surface of the sample.
5
6
7
8 Bottom figure shows the changes in composition gradient along the depth direction.
9
10
11 Dashed lines in the images indicate the LiSi ratio at each depth.

12
13
14 To measure the chemical composition of the samples summarized above, an XPS depth
15 profile was collected and is shown in Figure 2. This sample shows a gradient of
16
17 lithium/silicon with depth: the lithium concentration gradually decreases while the
18
19 silicon concentration gradually increases from surface to bulk. The resulting lithium-
20
21 silicon ratio ranges from Li_2Si to LiSi . In the future, it would be interesting to study Li_xSi
22
23
24 with a more homogeneous composition depth profile formed from inter-diffusion of
25
26 multilayered Li/Si samples. At the depth of ~50–150 nm, the Si 2p XPS peak has a low BE
27
28 of ~98 eV and the Li 1s peak has a metallic BE of 55 eV. This result, combined with the
29
30 negligible O 1s content, indicates the formation of lithium silicide. The XPS depth profile
31
32 also suggests that the lithium silicide thin film expanded compared to the original 50-nm
33
34 Si thin film, which is similar to the electrochemically lithiated silicon. Even though the
35
36 sample was stored in a glovebox for only 3 days before the XPS measurement, surface
37
38 oxygen contamination was inevitable. We also found that the surface of the lithium
39
40 silicide was contaminated with P and F due to electrolyte-related activities performed in
41
42 the same glovebox.
43
44
45
46
47
48
49
50
51
52
53
54
55
56
57
58
59
60

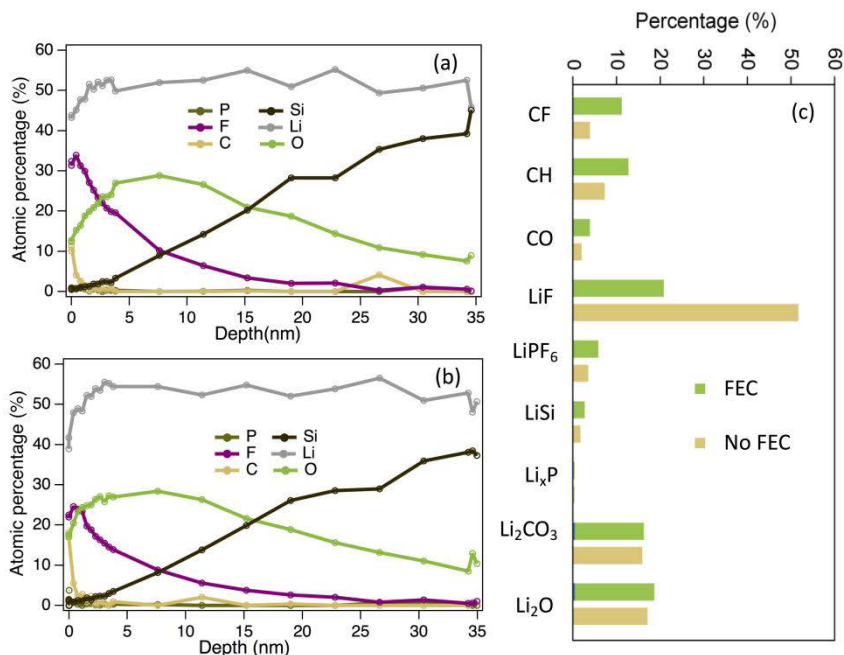


Figure 3. Composition depth profile of two Li_xSi samples treated by EC/DMC electrolyte (a) with FEC; (b) without FEC; (c) Composition analysis at the surface for EC/DMC electrolyte with FEC and without FEC.

To reveal the chemistry at the interface of the lithium silicide and electrolyte, lithium silicide film was exposed to two electrolytes (with and without FEC) immediately after deposition. The film was then gently washed with DMC before spectroscopic characterization. XPS spectra are shown in Figure S1. The XPS atomic percentage depth profiles are shown in Figure 3 for thin-film samples treated by electrolytes both with and without FEC. Large differences in F and O concentration were observed between the pristine and electrolyte-treated sample. F concentration increased and O concentration decreased after being treated with electrolyte. Generally, for both types of samples, the decomposition product layer has a composition that varies from the surface to bulk, with

1
2
3 the surface enriched in LiF, Li₂O, Li₂CO₃, and organic species. The F signal and C signal
4
5
6 decrease from the surface to bulk.
7

8
9 Significant differences are observed between decomposition products of the two
10
11 electrolytes at the near-surface layer. Electrolyte with FEC resulted in two times less F-
12
13 containing species at the surface (Figure 3c). Also, more C-containing species were
14
15 observed at the surface of the FEC decomposition products. One possible decomposition
16
17 mechanism is that FEC quickly breaks down on the surface of lithium silicide, generating
18
19 carbon monoxide or its precursor, F⁻ anion, and negatively charged C- and O-containing
20
21 fragments.²⁶ These fragments may undergo further reactions and affect the subsequent
22
23 decomposition of other solvents and salts. The SEI layer that grows on lithium silicide
24
25 can be described by the near-shore mechanism—where the SEI components aggregate in
26
27 the near-shore region—rather than by the “surface-growth mechanism,” which describes
28
29 the SEI formation on silicon where the SEI components progress until the SEI layer is
30
31 thick enough to prevent further electrolyte reduction.²⁷⁻²⁸ Note that even with the Li₂O at
32
33 the surface, the electrolyte was reduced by Li_xSi. Despite the difference in the depth
34
35 profile, these two samples (with and without FEC) share a similar thickness of SEI layer
36
37 (20–30 nm), defined as the depth at which the F signal disappears. As a reference, XPS
38
39 was also collected on an electrolyte-treated silicon wafer (Figure S2). We found that the
40
41 Si wafer surface was covered by a very thin (1-nm) residue, indicating that no chemical
42
43 reduction of electrolyte occurred at the silicon surface.
44
45
46
47
48
49
50
51
52
53
54
55
56
57
58
59
60

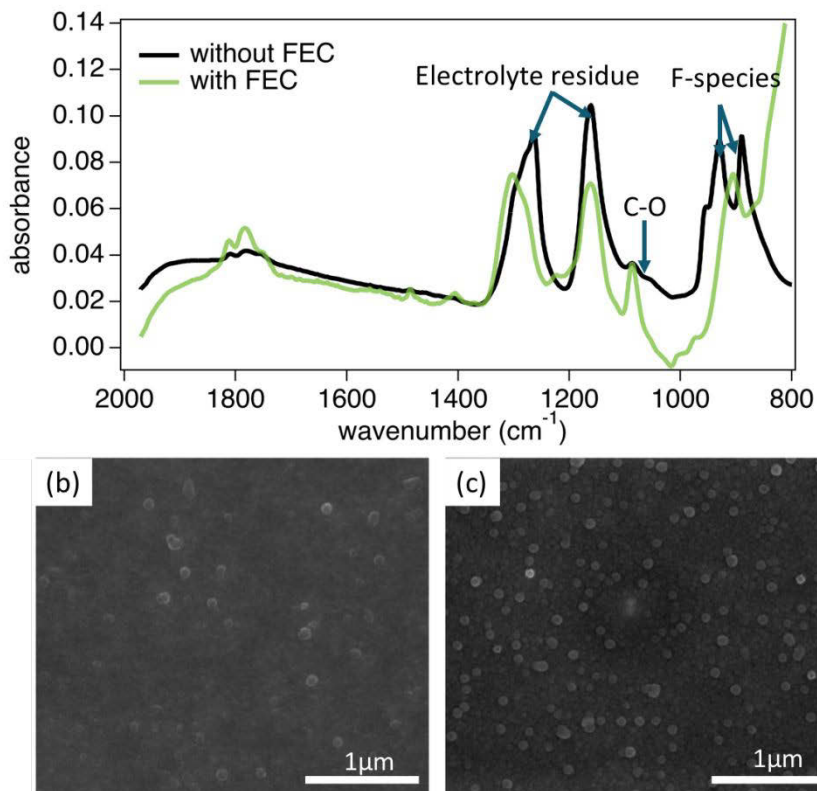


Figure 4. (a) ATR-FTIR spectra of the lithium silicide surface treated by EC/DMC electrolyte with and without FEC. Signals were normalized by signal strength of electrolyte residue. Scanning electron microscopy images of the electrode surface after EC/DMC electrolyte treatments (b) with FEC and (c) without FEC. Scale bar is 1 μm .

To gain additional insight into the chemistry of electrolyte reduction on lithium silicide, we measured ATR-FTIR spectra of the lithium silicide samples treated with two different electrolytes (Figure 4). We found that more F-containing species (P-F and LiF) are observed in the spectrum between 800 and 900 cm^{-1} for electrolyte with FEC, indicating that it helps to suppress the decomposition of LiPF_6 on lithium-rich surfaces. The

presence of FEC also increases the C-O signal at $1,084\text{ cm}^{-1}$, indicating that more organic species are formed. These differences in F species and carbonate species measured by ATR-FTIR are consistent with XPS data. Overall, this ATR-FTIR measurement combined with XPS results support the fact that electrolyte can be chemically reduced by lithium silicide. Scanning electron microscope images in Figures 4b and 4c show that the presence of the FEC electrolyte component led to a smoother surface compared to the electrolyte without FEC.

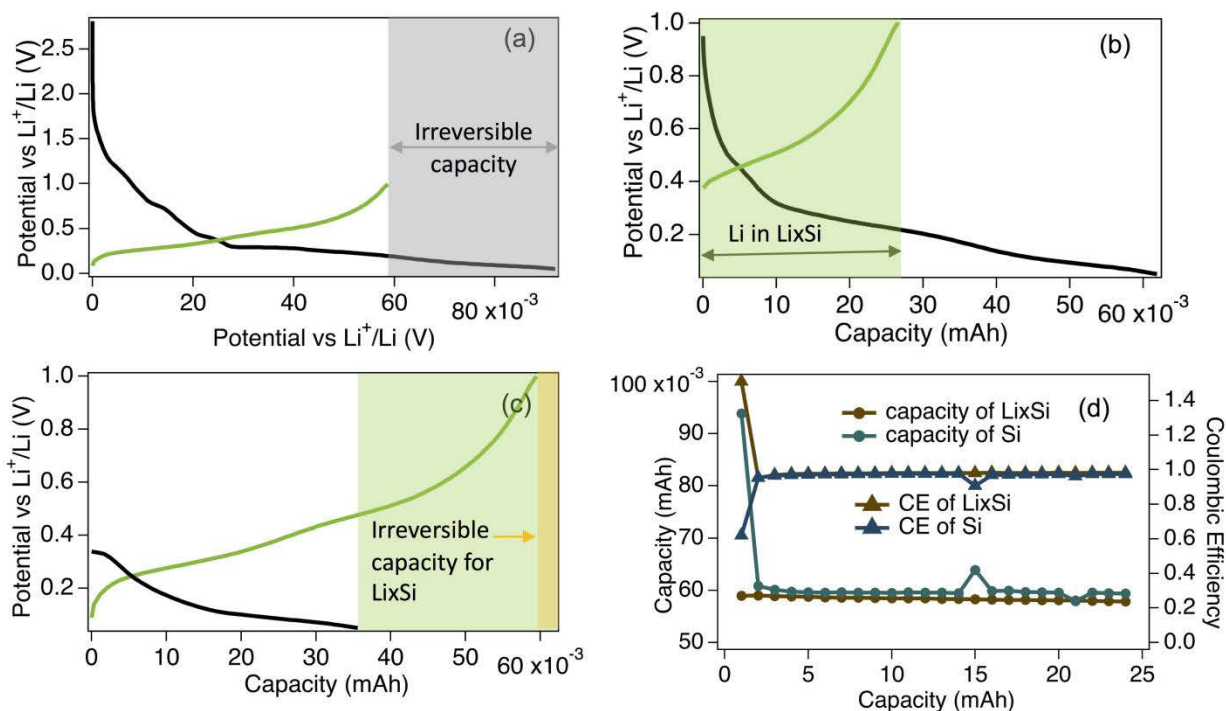


Figure 5. (a) Voltage profiles of Si thin film; (b) Voltage profiles of Li_xSi thin film; cell was discharged first; (c) Voltage profiles of Li_xSi ; cell was charged first; (d) cycling performance of Si and Li_xSi half-cell.

1
2
3 The first-cycle irreversible capacity was used to estimate how the surface lithium
4 potential would affect the SEI formation by comparing the planar amorphous silicon (50
5
6 nm) and lithium silicide thin films, both of which are expected to show no cracking
7
8 during the cycling. This methodology has also been used in previous studies.²⁹⁻³⁰ For this
9
10 purpose, the as-deposited Si and Li_xSi thin films were assembled into half cells in
11
12 EC/DMC electrolyte with FEC additive. The resulting first-cycle voltage profiles of the
13
14 reference silicon thin film and lithium silicide thin films are shown in Figure 5.
15
16 Irreversible capacity for silicon is usually calculated by subtracting the charge capacity
17
18 from discharge capacity (0.032 mAh in Figure 5a). To evaluate the irreversible capacity of
19
20 lithium silicide, two separate cells with the same electrode areas were prepared. First, we
21
22 determine how much lithium could be extracted from lithium silicide by charging the
23
24 first half-cell (Figure 5b). Second, we determine how much lithium could be added to
25
26 lithium silicide by discharging the second half-cell (Figure 5c). By adding how much
27
28 lithium could be extracted from the lithium silicide film from Figure 5b and how much
29
30 lithium could be added to lithium silicide from Figure 5c, we can deduce how much total
31
32 lithium is in the film after the first discharge. Then, irreversible capacity can be calculated
33
34 by subtracting the first charge capacity from the total lithium in the film, with the result
35
36 shown in the green rectangular in Figure 5c. The irreversible capacity (0.003 mAh, yellow
37
38 rectangle in Figure 5c) is negligible compared to silicon. This indicates that very little
39
40
41
42
43
44
45
46
47
48
49
50
51
52
53
54
55
56
57
58
59
60

1
2
3 irreversible capacity was lost due to SEI formation. The decomposition products on the
4
5
6 lithium silicide surface prevent further electrolyte reduction.
7

8
9 To put the results from our lithium silicide study into the context of more common
10
11 silicon studies, cycling performance measurements were compared for these samples,
12
13 with both cells discharged (lithiated) first. As shown in Figure 5d, lithium silicide showed
14
15 almost exactly the same cycling performance and columbic efficiency as silicon, with the
16
17 exception of the first cycle. This indicates that the SEI formed electrochemically on silicon
18
19 at the first cycle is as stable as the SEI formed chemically on lithium silicide. To
20
21 understand the role of different electrolyte components in this process, lithium silicide
22
23 cycling performance was evaluated with and without FEC (Figure S3). Little difference
24
25 could be seen from the first-cycle voltage profiles (Figure S3a), but a large difference was
26
27 observed in the cycling performance of thin films (Figure S3b). After 100 cycles, 93% of
28
29 the initial capacity was retained with the FEC component, whereas only 30% of capacity
30
31 was retained without the FEC component. These differences in cycling performance are
32
33 strongly correlated with the observation that the FEC results in less inorganic and more
34
35 organic phase formation on the surface (Figure 3), and this leads to a smoother and more
36
37 uniform surface (Figure 4). Correlation of these electrochemical and spectroscopic results
38
39 underscores the importance of FEC in the electrolyte reduction process during silicon
40
41 anode cycling.
42
43
44
45
46
47
48
49
50
51
52

53 54 **Conclusions** 55 56 57 58 59 60

1
2
3 In summary, we showed the chemical origin of SEI formation by electrolyte reduction
4
5 on lithium silicide. Lithium silicide thin films were synthesized by thermal evaporation
6
7 of lithium onto sputtered silicon thin film, with subsequent inter-diffusion between these
8
9 two layers. ATR-FTIR and XPS analyses of the surface of lithium silicide that was soaked
10
11 in electrolyte reveal the products of chemical reaction between lithium silicide and
12
13 electrolyte. The electrolyte composition affects the chemistry of electrolyte reduction and
14
15 results in more organic phases and fewer particulates when FEC is added. Lithium
16
17 silicide thin films exhibited negligible irreversible capacity loss compared to that of the
18
19 silicon anode. The negligible capacity loss due to SEI formation also suggests that the
20
21 decomposition product of electrolyte on lithium silicide prevented electrolyte reduction
22
23 during the first cycle. Furthermore, these two samples showed comparable cycling
24
25 performance: decomposition product on lithium silicide before the first cycle is
26
27 comparable to that SEI on Si formed after first discharge. Overall, these results reveal the
28
29 chemical origin of electrolyte reduction on lithium silicide, which is an important insight
30
31 for improving the calendar lifetime of Si-based Li-ion batteries. The results of this study
32
33 also suggest that developing an artificial SEI for silicon, as well as application of
34
35 prelithiated silicon anodes, can be viable routes for increasing the performance of such
36
37 batteries.
38
39
40
41
42
43
44
45
46
47
48
49
50
51
52
53
54
55

56 **Supporting Information**

57
58
59
60

1
2
3 Supporting information including XPS of electrolyte-treated silicon wafer, depth profile
4
5
6 of the silicon surface, electrochemical cycling of lithium silicide with different
7
8
9 electrolyte (PDF)

11 AUTHOR INFORMATION

15 **Corresponding Author**

16
17
18 Andriy Zakutayev, andriy.zakutayev@nrel.gov
19
20
21

22 **Present Addresses**

23
24
25 Materials Science Center, National Renewable Energy Laboratory, Golden, CO, 80401,
26
27
28 USA
29
30

31 **Author Contributions**

32
33
34 The manuscript was written through contributions of all authors. All authors have
35
36
37 given approval to the final version of the manuscript.
38
39
40

41 **ACKNOWLEDGMENT**

42
43
44 This work was authored by the National Renewable Energy Laboratory, operated
45
46 by Alliance for Sustainable Energy, LLC, for the U.S. Department of Energy (DOE) under
47
48 Contract No. DE-AC36-08GO28308. Funding provided by the Vehicle Technologies
49
50 Office, Hybrid Electric Systems Program. David Howell (Manager), Battery R&D, and
51
52 Brian Cunningham and Peter Faguy (Technology Managers) at the U.S. Department of
53
54
55
56
57
58
59
60

Pursuant to the DOE Public Access Plan, this document represents the authors' peer-reviewed, accepted manuscript. The published version of the article is available from the relevant publisher.

Energy, Office of Energy Efficiency and Renewable Energy, are gratefully acknowledged.

The views expressed in the article do not necessarily represent the views of the DOE or the U.S. Government.

Reference

1. Sharma, R. A.; Seefurth, R. N., Thermodynamic Properties of the Lithium-Silicon System. *J. Electrochem. Soc.* **1976**, *123*, 1763-1768.
2. Boukamp, B. A.; Lesh, G. C.; Huggins, R. A., All-Solid Lithium Electrodes with Mixed-Conductor Matrix. *J. Electrochem. Soc.* **1981**, *128*, 725-729.
3. Nie, M.; Abraham, D. P.; Chen, Y.; Bose, A.; Lucht, B. L., Silicon Solid Electrolyte Interphase (Sei) of Lithium Ion Battery Characterized by Microscopy and Spectroscopy. *J. Phys. Chem. C* **2013**, *117*, 13403-13412.
4. Jin, Y.; Kneusels, N.-J.; Marbella, L.; Kim, G.; Castillo-Martínez, E.; Magusin, P. C. M. M.; Grey, C. P., (Invited) Nmr Studies of Sei Coatings on Silicon. *Meeting Abstracts* **2017**, *MA2017-02*, 146-146.
5. Schroder, K. W.; Celio, H.; Webb, L. J.; Stevenson, K. J., Examining Solid Electrolyte Interphase Formation on Crystalline Silicon Electrodes: Influence of Electrochemical Preparation and Ambient Exposure Conditions. *J. Phys. Chem. C* **2012**, *116*, 19737-19747.

- 1
2
3 6. Veith, G. M.; Doucet, M.; Sacci, R. L.; Vacaliuc, B.; Baldwin, J. K.; Browning, J. F.,
4
5
6 Determination of the Solid Electrolyte Interphase Structure Grown on a Silicon
7
8
9 Electrode Using a Fluoroethylene Carbonate Additive. *Sci. Rep.* **2017**, *7*, 6326.
10
- 11 7. Shi, F.; Ross, P. N.; Somorjai, G. A.; Komvopoulos, K., The Chemistry of
12
13
14 Electrolyte Reduction on Silicon Electrodes Revealed by in Situ Atr-Ftir Spectroscopy. *J.*
15
16
17 *Phys. Chem. C* **2017**, *121*, 14476-14483.
18
- 19 8. Horowitz, Y.; Han, H.-L.; Ross, P. N.; Somorjai, G. A., In Situ Potentiodynamic
20
21
22 Analysis of the Electrolyte/Silicon Electrodes Interface Reactions - a Sum Frequency
23
24
25 Generation Vibrational Spectroscopy Study. *J. Am. Chem. Soc.* **2016**, *138*, 726-729.
26
- 27 9. Steinhauer, M.; Stich, M.; Kurniawan, M.; Seidlhofer, B.-K.; Trapp, M.; Bund, A.;
28
29
30 Wagner, N.; Friedrich, K. A., In Situ Studies of Solid Electrolyte Interphase (Sei)
31
32
33 Formation on Crystalline Carbon Surfaces by Neutron Reflectometry and Atomic Force
34
35
36 Microscopy. *ACS Appl. Mater. & Interfaces* **2017**, *9*, 35794-35801.
37
- 38 10. Zhao, J.; Lu, Z.; Liu, N.; Lee, H.-W.; McDowell, M. T.; Cui, Y., Dry-Air-Stable
39
40
41 Lithium Silicide–Lithium Oxide Core–Shell Nanoparticles as High-Capacity
42
43
44 Prelithiation Reagents. *Nat. Commun.* **2014**, *5*, 5088.
45
- 46 11. Li, X.; Kersey-Bronec, F. E.; Ke, J.; Cloud, J. E.; Wang, Y.; Ngo, C.; Pylypenko, S.;
47
48
49 Yang, Y., Study of Lithium Silicide Nanoparticles as Anode Materials for Advanced
50
51
52 Lithium Ion Batteries. *ACS Appl. Mater. & Interfaces* **2017**, *9*, 16071-16080.
53
54
55
56
57
58
59
60

- 1
2
3
4
5
6
7
8
9
10
11
12
13
14
15
16
17
18
19
20
21
22
23
24
25
26
27
28
29
30
31
32
33
34
35
36
37
38
39
40
41
42
43
44
45
46
47
48
49
50
51
52
53
54
55
56
57
58
59
60
12. Zhang, X.; Kostecki, R.; Richardson, T. J.; Pugh, J. K.; Ross, P. N., Electrochemical and Infrared Studies of the Reduction of Organic Carbonates. *J. Electrochem. Soc.* **2001**, *148*, A1341-A1345.
13. Leung, K.; Rempe, S. B.; Foster, M. E.; Ma, Y.; Martinez del la Hoz, J. M.; Sai, N.; Balbuena, P. B., Modeling Electrochemical Decomposition of Fluoroethylene Carbonate on Silicon Anode Surfaces in Lithium Ion Batteries. *J. Electrochem. Soc.* **2014**, *161*, A213-A221.
14. Jaumann, T., et al., Lifetime Vs. Rate Capability: Understanding the Role of FEC and VC in High-Energy Li-Ion Batteries with Nano-Silicon Anodes. *Energy Storage Mater.* **2017**, *6*, 26-35.
15. Xu, C.; Lindgren, F.; Philippe, B.; Gorgoi, M.; Björefors, F.; Edström, K.; Gustafsson, T., Improved Performance of the Silicon Anode for Li-Ion Batteries: Understanding the Surface Modification Mechanism of Fluoroethylene Carbonate as an Effective Electrolyte Additive. *Chem. Mater.* **2015**, *27*, 2591-2599.
16. Markevich, E.; Salitra, G.; Aurbach, D., Fluoroethylene Carbonate as an Important Component for the Formation of an Effective Solid Electrolyte Interphase on Anodes and Cathodes for Advanced Li-Ion Batteries. *ACS Energy Lett.* **2017**, *2*, 1337-1345.
17. Schroder, K.; Alvarado, J.; Yersak, T. A.; Li, J.; Dudney, N.; Webb, L. J.; Meng, Y. S.; Stevenson, K. J., The Effect of Fluoroethylene Carbonate as an Additive on the Solid

- 1
2
3 Electrolyte Interphase on Silicon Lithium-Ion Electrodes. *Chem. Mater.* **2015**, *27*, 5531-
4
5
6 5542.
7
8
9 18. Li, Q.; Liu, X.; Han, X.; Xiang, Y.; Zhong, G.; Wang, J.; Zheng, B.; Zhou, J.; Yang,
10
11 Y., Identification of the Solid Electrolyte Interface on the Si/C Composite Anode with
12
13 Fec as the Additive. *ACS Appl. Mater. & Interfaces* **2019**, *11*, 14066-14075.
14
15
16 19. Young, B. T.; Heskett, D. R.; Nguyen, C. C.; Nie, M.; Woicik, J. C.; Lucht, B. L.,
17
18 Hard X-Ray Photoelectron Spectroscopy (Haxpes) Investigation of the Silicon Solid
19
20 Electrolyte Interphase (Sei) in Lithium-Ion Batteries. *ACS Appl. Mater. & Interfaces* **2015**,
21
22 *7*, 20004-20011.
23
24
25
26 20. Martinez de la Hoz, J. M.; Leung, K.; Balbuena, P. B., Reduction Mechanisms of
27
28 Ethylene Carbonate on Si Anodes of Lithium-Ion Batteries: Effects of Degree of
29
30 Lithiation and Nature of Exposed Surface. *ACS Appl. Mater. & Interfaces* **2013**, *5*, 13457-
31
32 13465.
33
34
35
36 21. Hankins, K.; Soto, F. A.; Balbuena, P. B., Insights into the Li Intercalation and SEI
37
38 Formation on Lisi Nanoclusters. *J. Electrochem. Soc.* **2017**, *164*, E3457-E3464.
39
40
41
42 22. Strauß, F.; Hüger, E.; Heitjans, P.; Trouillet, V.; Bruns, M.; Schmidt, H., Li-Si Thin
43
44 Films for Battery Applications Produced by Ion-Beam Co-Sputtering. *RSC Adv.* **2015**, *5*,
45
46 7192-7195.
47
48
49
50 23. Kuwata, H.; Sonoki, H.; Matsui, M.; Matsuda, Y.; Imanishi, N., Surface Layer and
51
52 Morphology of Lithium Metal Electrodes. *Electrochem.* **2016**, *84*, 854-860.
53
54
55
56
57
58
59
60

- 1
2
3 24. Schmid, M.; Steinrück, H. P.; Gottfried, J. M., A New Asymmetric Pseudo-Voigt
4
5
6 Function for More Efficient Fitting of Xps Lines. *Surf. Interface Anal.* **2014**, *46*, 505-511.
7
8
9 25. Xu, Y.; Stetson, C.; Wood, K.; Sivonxay, E.; Jiang, C.; Teeter, G.; Pylypenko, S.;
10
11 Han, S.-D.; Persson, K. A.; Burrell, A.; et. al. Mechanical Properties and Chemical
12
13 Reactivity of Li_xSiO_y Thin Films. *ACS Appl. Mater. & Interfaces* **2018**, *10*, 38558-38564.
14
15
16 26. Sprowl, L. H.; Árnadóttir, L.; Chan, M. K. Y., Surface Sensitivity of
17
18 Fluoroethylene Carbonate Breakdown on Lithium Silicide Surfaces. *Meeting Abstracts*
19
20
21 **2017**, *MA2017-02*, 183-183.
22
23
24 27. Ushirogata, K.; Sodeyama, K.; Futera, Z.; Tateyama, Y.; Okuno, Y., Near-Shore
25
26 Aggregation Mechanism of Electrolyte Decomposition Products to Explain Solid
27
28 Electrolyte Interphase Formation. *J. Electrochem. Soc.* **2015**, *162*, A2670-A2678.
29
30
31
32 28. Leung, K., Predicting the Voltage Dependence of Interfacial Electrochemical
33
34 Processes at Lithium-Intercalated Graphite Edge Planes. *Phys. Chem. Chem. Phys.* **2015**,
35
36
37 *17*, 1637-1643.
38
39
40 29. Nadimpalli, S. P. V.; Sethuraman, V. A.; Dalavi, S.; Lucht, B.; Chon, M. J.; Shenoy,
41
42
43 V. B.; Guduru, P. R., Quantifying Capacity Loss Due to Solid-Electrolyte-Interphase
44
45 Layer Formation on Silicon Negative Electrodes in Lithium-Ion Batteries. *J. Power*
46
47
48 *Sources* **2012**, *215*, 145-151.
49
50
51
52
53
54
55
56
57
58
59
60

- 1
2
3 30. Michan, A. L.; Divitini, G.; Pell, A. J.; Leskes, M.; Ducati, C.; Grey, C. P., Solid
4
5
6 Electrolyte Interphase Growth and Capacity Loss in Silicon Electrodes. *J. Am. Chem. Soc.*
7
8
9 **2016**, *138*, 7918-7931.
10
11
12
13
14
15
16
17
18
19
20
21
22
23
24
25
26
27
28
29
30
31
32
33
34
35
36
37
38
39
40
41
42
43
44
45
46
47
48
49
50
51
52
53
54
55
56
57
58
59
60

TOC Graphic

